Cerebral Cortex, 2018; 1–13

doi: 10.1093/cercor/bhy043
Original Article

ORIGINAL ARTICLE

Terminal Arbors of Callosal Axons Undergo Plastic Changes in Early-Amputated Rats

Carlomagno Pacheco Bahia[1,2,†], Rodrigo Jorge Vianna-Barbosa[1,†], Fernanda Tovar-Moll[1,3] and Roberto Lent[1]

[1]Institute of Biomedical Sciences, Federal University of Rio de Janeiro, CEP 21941-902 Rio de Janeiro (RJ), Brazil, [2]Institute of Health Sciences, Federal University of Pará, CEP 66075-110 Belém (PA), Brazil and [3]D'Or Institute of Research and Education, CEP 22281-100 Rio de Janeiro (RJ), Brazil

Address correspondence to Roberto Lent, Institute of Biomedical Sciences, Federal University of Rio de Janeiro, Av. Carlos Chagas 373, bl. F, 1st Floor, rm 31, CEP 21941-902 Rio de Janeiro (RJ), Brazil. E-mail: rlent@icb.ufrj.br

[†]Carlomagno Pacheco Bahia and Rodrigo Jorge Vianna-Barbosa contributed equally to the present work

Abstract

Sensory information is processed in specific brain regions, and shared between the cerebral hemispheres by axons that cross the midline through the corpus callosum. However, sensory deprivation usually causes sensory losses and/or functional changes. This is the case of people who suffered limb amputation and show changes of body map organization within the somatosensory cortex (S1) of the deafferented cerebral hemisphere (contralateral to the amputated limb), as well as in the afferented hemisphere (ipsilateral to the amputated limb). Although several studies have approached these functional changes, the possible finer morphological alterations, such as those occurring in callosal axons, still remain unknown. The present work combined histochemistry, single-axon tracing and 3D microscopy to analyze the fine morphological changes that occur in callosal axons of the forepaw representation in early amputated rats. We showed that the forepaw representation in S1 was reduced in the deafferented hemisphere and expanded in the afferented side. Accordingly, after amputation, callosal axons originating from the deafferented cortex undergo an expansion of their terminal arbors with increased number of terminal boutons within the homotopic representation at the afferented cerebral hemisphere. Similar microscale structural changes may underpin the macroscale morphological and functional phenomena that characterize limb amputation in humans.

Key words: 3D axon reconstruction, amputation, corpus callosum, morphological plasticity, somatosensory cortex

Introduction

The cerebral cortex has a great potential for neuroplasticity along its lifespan, undergoing adaptive changes after intrinsic and extrinsic influences from early development until adulthood. This adaptive plasticity can be observed in all primary sensory brain areas after different kinds of deprivation, and falls into at least 2 distinct categories (Lee and Whitt 2015): (1) recruitment of the deprived sensory cortex for processing the intact senses, known as "cross-modal recruitment" or "cross-modal plasticity" and (2) experience-dependent refinement of the spared sensory cortices, referred to as "compensatory plasticity" (Payne 1996; Lent and Tovar-Moll 2015). In both cases, morphological changes take place both at the neuronal level, including axonal and dendritic arbors, and at the areal level, including topographic representation maps (Buonomano and Merzenich 1998; Fox 2002).

When sensory deprivation occurs during the most sensitive (critical) period of neural development, larger changes take place, involving not only local circuits but also long-range pathways as well (Bowlus et al. 2003; Staudt et al. 2004). This is the

case of the thalamocortical pathway (Fox 2002) and of interhemispheric connections (Pelled et al. 2007; Suarez et al. 2014). Long-distance plasticity after sensory deprivation can also involve the reorganization of homologous areas in the nondeprived hemisphere (Foeller and Feldman 2004; Petersen 2007). Thus, morphological and functional changes occur not only in the sensory maps of the cerebral hemisphere contralateral to peripheral deprivation (heretofore named deafferented hemisphere), but also in the one ipsilateral to peripheral deprivation (afferented hemisphere) (Koralek et al. 1990; Simões et al. 2012).

In cases of limb amputation, and consequently peripheral nerves transection, the central targets are not only limited to the somatosensory cortical regions but also extend to the motor cortex, with expanded representation of the body parts adjacent to the amputated limb (Welker and Van der Loos 1986; Catania 2005; Catania and Henry 2006). Within the primary somatosensory area (S1), amputation can promote functional changes that have been related to phantom sensations (Chen et al. 2012), such as expansion of the cortical representation of the stump (Karl et al. 2001) and a corresponding increase in interhemispheric connections therein (Ramachandran et al. 1992; Hua et al. 2012).

Most interhemispheric connections cross the midline through the corpus callosum, which is the major neural pathway connecting cortical cerebral areas of both hemispheres (Aboitiz et al. 1992a, 1992b; Bloom and Hynd 2005). In S1, most anatomical and functional studies performed to date have demonstrated more abundant callosal connections in the areas of representation of medial body portions (Jones and Powell 1968; Pandya et al. 1971; Akers and Killackey 1979; Ivy et al. 1979). However, callosal projections representing peripheral body parts lateral to the midline (such as the limb extremities) have also been described in man (Maldjian et al. 1999), monkey (Pandya et al. 1971; Manzoni et al. 1986), cat (Caminiti et al., 1979), and rodents such as the mouse (Ivy et al. 1979) and the agouty (Rocha et al. 2007).

Several studies propose that the corpus callosum provides a pathway for homologous interhemispheric modulation of cortical areas, possibly through a balance between excitation and inhibition (reviewed in Bloom and Hynd 2005; Innocenti 2009; and van der Knaap and van der Ham 2011). The relevance of callosal connections to the issue of cortical plasticity after limb amputation is that their modulatory effects in the opposite hemisphere may be at the root of the mechanisms explaining reduction and expansion of representation fields, as well as the corresponding phantom phenomena.

Indeed, functional magnetic resonance imaging (fMRI) of amputated humans evidenced a reduction of the fractional anisotropy in the corpus callosum, suggesting alterations in the callosal microstructure (Simões et al. 2012), together with an expansion of both contralateral and ipsilateral representations of body parts in the cerebral cortex. Accordingly, recent work from our group has indicated that amputation in adult animals causes changes in myelination of callosal fibers at the midline (Vianna-Barbosa et al. 2017). Based on these findings, we reasoned that these phenomena may also be reflected onto even more subtle morphological changes at the single-axon terminal level. To clarify this possibility, we have developed an animal model of great plasticity potential—early, forelimb-amputated rats—and describe both the areal changes in the cerebral cortex and the fine morphology of callosal axons that connect the somatosensory representation of the forepaw. By use of 3D reconstructions of labeled single-axons, we show an enlargement of axonal telodendria with an increase in the number of synapses, that can be related with other phenomena reported at a more systemic level of analysis.

Materials and Methods

Male adult Wistar rats ($n = 24$) obtained from the central animal facility of the Institute of Biomedical Sciences, were submitted to experimental procedures following the "Guide for the Care and Use of Laboratory Animals" (NIH publication, No. 86-23, revised 1985) and previously approved by the local Ethics Committee for the use of animals (Protocol Number 046/2015). All efforts were made to avoid animal suffering and to reduce the number of animals used.

Forelimb Amputation

Newborn pups underwent forelimb amputation (Fig. 1A) by using a previously described approach (Lane et al. 1995). Briefly, the pups (<12 h old) were anesthetized by 5 min hypothermia. After testing for the absence of pain reflexes, the right forelimb was cut at the level of the elbow, and the stump was electrocauterized to control for bleeding, after infiltration with a local

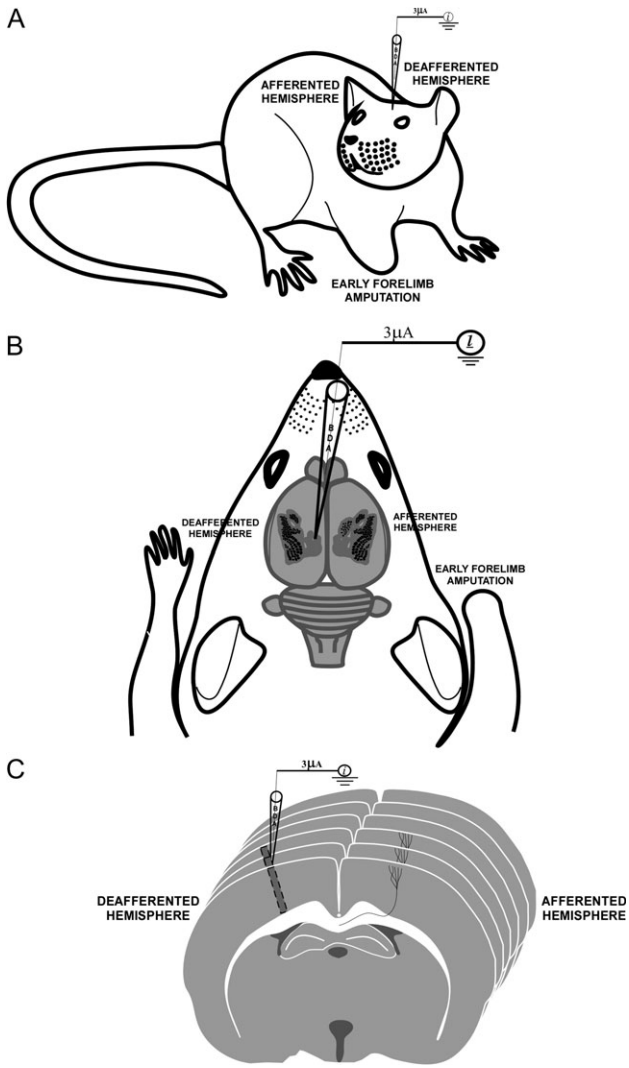

Figure 1. Outline of the experiment as described in the text. (*A*) The amputated animal model. (*B*) The location of iontophoretic tracer microinjections into the deafferented hemisphere, as well as the afferented hemisphere where labeled axons were studied, both with the somatotopic maps delineated therein. (*C*) The serial sections obtained from the brain, and 3D reconstruction of a callosal axon, as an example.

anesthetic (0.7% bupivacaine, Nortec Quimica, Brazil). The skin was then closed with cyanoacrylate adhesive, the animals were rewarmed, returned to their mothers, and maintained under care in the vivarium until 3 months old, at which age (P90–P120) the subsequent protocols were performed.

Electrophysiological Recordings

Electrophysiological recordings were performed to locate the somatotopic representation of the forelimb within S1 of each animal, and therefore better orient the injection of axonal tracer. One day before surgery, all animals (0.30–0.35 kg) were premedicated intramuscularly (IM) with 1.0 mg/kg of dexamethasone (Decadron, Prodome, Brazil) to prevent brain edema, and with 1.0 mg/kg IM vitamin K (Kanakion, Roche, Brazil) to avoid excessive bleeding during surgery. Immediately before surgery, the animals received 0.1 mg/kg IM of atropine sulfate (Ariston, Brazil) and anesthesia was induced with a mixture of 100 mg/kg IM of ketamine (Ketalar, Parker, Brazil) and with 5 mg/kg IM of xylazine (Rompun, Bayer, Brazil). If necessary, supplementary doses of ketamine were provided during the surgical procedure. Body temperature was monitored and maintained at about 37 °C with the help of a heating pad (Homeothermic Blanket Control, Harvard Bioscience, USA).

Two groups of animals were utilized for axonal tracing: (1) amputated (AMP, $n = 6$) and (2) nonamputated controls (CTRL, $n = 6$). For both groups, the head of the animal was securely placed in a stereotaxic apparatus (Insight, Brazil) and a small craniotomy was made at the stereotactic coordinates AP = –2.0 and ML = 5.0, which correspond approximately to the forepaw representation in S1 (Paxinos et al. 1980; Paxinos and Watson 2007). Then, extracellular multiunit electrophysiological responses after peripheral tactile stimulation were recorded within S1 of the left cerebral cortex (Fig. 1B). In each case, the forepaw (CTRL) or stump (AMP) was mechanically stimulated by light touches with a brush.

Tungsten microelectrodes were employed (9–12 MΩ at 1 kHz, FHC, USA) to record multiunit potentials which were amplified, band-pass filtered between 1 and 3 kHz (ME04011, FHC, USA) and sent to a notebook running the software Audacity (SourceForge.net). Responses from tactile stimulation of the forepaw or stump were identified and their cortical representation localized and translated into stereotaxic coordinates. By the end of the recording session, the electrode was removed and a glass capillary was positioned in the same place for neuronal tract-tracer injection.

Axonal Tracer Injections and Labeling

In all the 12 animals (AMP and CTRL groups), we performed a single iontophoretic microinjection of 10% Biotinylated Dextran Amine 10 KDa (BDA, Molecular Probes, USA), diluted in phosphate buffer saline (PBS, pH 7.4, 0.1 M). Microinjections were made through a glass capillary (20–30 μm internal tip diameter) inserted contralaterally to the amputation side (left cerebral hemisphere, Fig. 1B), using stereotaxic coordinates previously determined by electrophysiological recording of the forepaw and stump representation in the left hemisphere of both experimental groups (–1 mm posterior and 3 mm lateral to bregma). Immediately after the electrophysiological identification of the correct position of the forepaw S1 representation at the cortical surface, positive current pulses of 5 μA (7 s ON, 7 s OFF) over 3–5 min were applied with a current source (Stoelting, USA) on the 10% Biotinylated Dextran Amine 10 KDa solution. By the end of the surgery, the cerebral cortex was covered with gelfoam (Absorbable Gelatin, Pharmacia, Brazil) and the cranial flap was placed back and sealed with acrylic (Acrylic, JET, Brazil). The skin was then sutured and treated with bactericidal cream (Nebacetin, Chemical BYK, Brazil). Additionally, we applied an extra-dose of 0.33 mL of antibiotic (Pentabiotic, Roche, Brazil) to prevent infections. After recovering from the anesthetic state, the animals were then returned to their cages with food and water ad libitum.

After 15 days, they were anesthetized with a lethal dose of ketamine and perfused transcardially with PBS followed by 4% paraformaldehyde in phosphate buffer (PF, pH 7.4, 0.1 M). The brains were removed from the skulls and cut coronally with a vibratome (Leica VT 100 S, Germany) into serial 150 μm-thick sections. The sections were washed 3 times for 20 min each in PBS and once in a solution of 3% Triton X-100 in PBS, before being incubated overnight in the avidin/biotin/peroxidase complex (ABC, diluted 1:200; Vector Laboratories, USA), at room temperature under constant agitation. Peroxidase labeling was obtained by reaction with diaminobenzidine (Sigma, USA) intensified with nickel ammonium sulfate (Shu et al. 1988). Finally, sections were dehydrated in rising concentrations of alcohols, cleared in xylene, mounted onto glass slides and coverslipped with Entellan (Merck, Germany).

Cytochrome Oxidase Histochemistry

In 12 additional animals (AMP, $n = 6$; CTRL, $n = 6$), we used cytochrome oxidase (CO) activity to label the whole somatotopic map in S1 (Wong-Riley 1989). For that purpose, the cerebral cortex of each hemisphere was flattened between 2 glass slides within a 4% paraformaldehyde solution, to allow the definition of comparable tangential planes for all cortices. Serial tangential sections, 50 μm-thick, were cut with a vibratome (Leica VT 100 S, Germany), and incubated in a solution containing 0.03% cytochrome C (Sigma, USA), 0.02% catalase (Sigma, USA) and 0.05% diaminobenzidine (Sigma, USA) in 0.1 M PBS. Development of the CO reaction was monitored regularly under microscopic observation and interrupted when the signal/background level was deemed satisfactory.

By careful examination at the microscope, 5 serial tangential sections comprising layer IV were selected for the reconstruction of S1 topographic map, as described below. For a correct reconstruction, the blood vessels pattern was used to align adjacent sections, and the shrinkage correction factor provided by the reconstruction software was used to minimize size changes that might have occurred during the histological procedures.

Morphometric Analysis and 3D Reconstruction

Twelve completely labeled callosal axons were selected from the animals injected with BDA (AMP, $n = 6$; CTRL, $n = 6$; 1 axon per animal), and reconstructed anterogradely from the midline until their terminal endings at the target hemisphere (left hemisphere in CTRL; afferented hemisphere in AMP, heretofore named AMP_{aff}; Fig. 1C). They were reconstructed blindly by different coauthors, directly from coronal sections (3 or 4 150 μm-thick serial sections for each axon), using a ×60 oil immersion objective of an Eclipse 90i microscope (Nikon, Japan) equipped with a high-resolution camera (MBF Bioscience, USA) and a 3D-motorized stage MAC5000 (MBF Bioscience, USA). The devices were connected to a PC running the Neurolucida software (MBF Bioscience, USA), thereby allowing recording and analysis of x, y, and z coordinates of digitized points, with correction for tissue shrinkage factor in the Z-axis (150 μm from the original

thickness and 50 μm thick from the mounted tissue with a shrinkage factor of 3) to match up the serial sections and recover the original data. After careful microscope inspection of the histological slides, only completely labeled callosal axons were digitized. Axon segments with cut ends were not included in the sample. Photomicrographs were made with a digital camera attached to the microscope, and brightness and contrast of the pictures were adjusted offline with Canvas XII (ACDC, USA).

Quantification and Statistical Analysis

In sections stained with CO histochemistry, we calculated the volume of forepaw representation in S1 of CTRL hemispheres, AMP deafferented (AMP_{deaff}) hemisphere and AMP afferented (AMP_{aff}) hemisphere. We also quantified the volume of barrels within the forepaw representation, and volumes of the forepaw representations and of barrels therein were blindly 3D-reconstructed using the Neurolucida Systems (MBF Bioscience, USA). The above volumes were computed by the software, taking cone-like figures drawn between each surface map from the most superficial section to the deepest one containing layer IV (MBF Bioscience, USA). In sections stained with BDA, the following morphometric parameters of axon terminals were analyzed in the cortical target region of callosal connections of S1 forepaw representation (Aguiar et al. 2013): area (total area contained within the boundary of the most external points of the arbor), volume (volume of a convex polygon obtained by connecting the tips of the most distal points of adjacent processes), surface (estimate of the arbor area represented at the cortical surface), perimeter (total length of the axon contour, either open or closed, that takes the Z positions of the coordinates into account), axonal axis orientation and scattering of axonal arbors (size of the axon branched arbor as a solid polygon delimitated by the tips of the distal axons segments). Additionally, we counted the total number of boutons "en passant" and boutons "terminaux". Reconstructed axons were selected after detailed microscope inspection, in order to verify that BDA labeling was complete, filling entirely the axon and its branches with no discontinuities or fragments. Values for these morphometric parameters were expressed as box-plot graphs and compared between 2 groups using Student's t test or across different groups using analysis of variance (ANOVA) and the Tukey post hoc test, with $\alpha = 0.05$.

Results

Forepaw Representation in S1 is Reduced in Deafferented and Expanded in Afferented Hemispheres After Amputation

CO labeling of the S1 forepaw representation (Fig. 2) and 3D reconstruction analysis (Fig. 3) demonstrated alterations in S1 forepaw representation in both cerebral hemispheres of the animals amputated at day of birth (P0).

Statistical analysis showed significant differences in volume of the S1 forepaw representation between CTRL, AMP_{deaff} and AMP_{aff} hemispheres ($F = 12.66$; $P < 0.01$). As shown in Figure 3, average forepaw representation volume is larger in the AMP_{aff} hemispheres ($5.256\,\mu m^3 \pm 0.513$; $P < 0.05$) and smaller in the AMP_{deaff} ones ($1.845\,\mu m^3 \pm 0.568$; $P < 0.006$) when compared with CTRL hemispheres (Fig. 3A). Similarly, the average volume of barrels within the forepaw representation in S1 of AMP_{aff} hemispheres was larger ($2.366\,\mu m^3 \pm 0.304$) than that in the CTRL hemispheres ($1.532\,\mu m^3 \pm 0.261$; $P < 0.05$). On the other hand, no barrels were labeled by CO in the S1 forepaw representation of the AMP_{deaff} hemispheres (Fig. 3B). Interestingly, the neighboring lower lip S1 representation of the AMP_{deaff} hemispheres ($4.985\,\mu m^3 \pm 0.159$) was expanded as compared with CTRL ($2.983\,\mu m^3 \pm 0.637$; $P < 0.05$). However, statistical significance was not reached between AMP_{aff} and CTRL hemispheres (Fig. 3C).

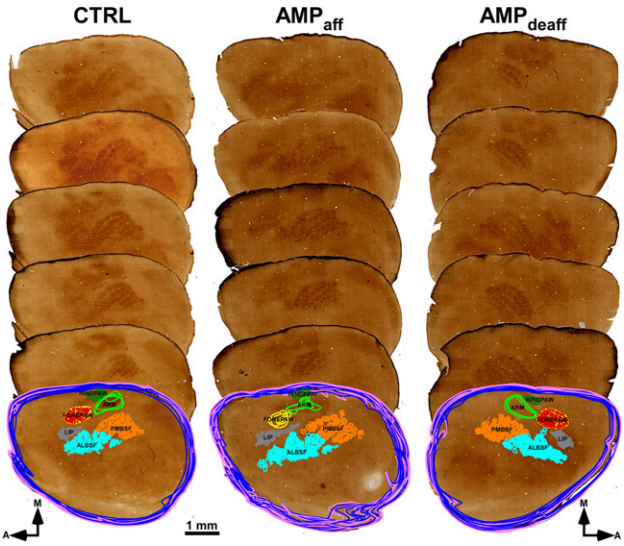

Figure 2. Serial horizontal sections, stained for cytochrome oxidase histochemistry, showing the somatotopic details of rat S1 for the 3 experimental groups. The lower sections show the stack of drawings made for all sections. CTRL: control group; AMP_{aff}: afferented hemisphere of amputees; AMP_{deaff}: deafferented hemisphere. Purple and pink contours depict the pial upper and lower surface of each section, respectively; light blue represents the barrels of the anterolateral barrel subfield (ALBSF); orange shows barrels of the posteromedial barrel subfield (PMBSF); grey depicts barrels of lower lip; yellow is for forepaw contours; light and dark green represent forearm and hindpaw, respectively.

Single Callosal Axons From the Forepaw Representation can be Followed From Midline Until Their Contralateral Terminal Field

All BDA iontophoretic microinjections were confined to S1 forepaw representation of AMP_{deaff} hemispheres as shown by double labeling in horizontal sections with both BDA and CO histochemistry reactions (Fig. 4). Anterograde projections were shown to reach other regions in the same cerebral hemisphere associated with areas secondary somatosensory (S2), parietal ventral (PV), and parietal rhinal (PR) (Fig. 4A), but also crossed the callosal midline at the expected sector of the callosal body (Fig. 4B) and formed a terminal field contralaterally within the homotopic forepaw region of S1 (black arrowhead in Fig. 4C).

At the center of the tracer microinjection (indicated by the pipette trajectory) a dense black central core of BDA deposit was seen (Fig. 5A,C), varying from 200 to 400 μm diameter, surrounded by labeled cell bodies and axonal segments spanning from layers II/III to VI (Fig. 5C). Cortical layers were rendered visible by background peroxidase activity (Fig. 5A,C). The terminal segments of callosal axons projecting from deafferented S1 could be seen within the contralateral cortex at the homotopic S1 forepaw representation (Fig. 5B), extending along all cortical layers and restricted to S1 (Fig. 5D).

3D reconstructions of single axons show clearly their whole arbors, and allow identification of boutons (Fig. 6). As shown

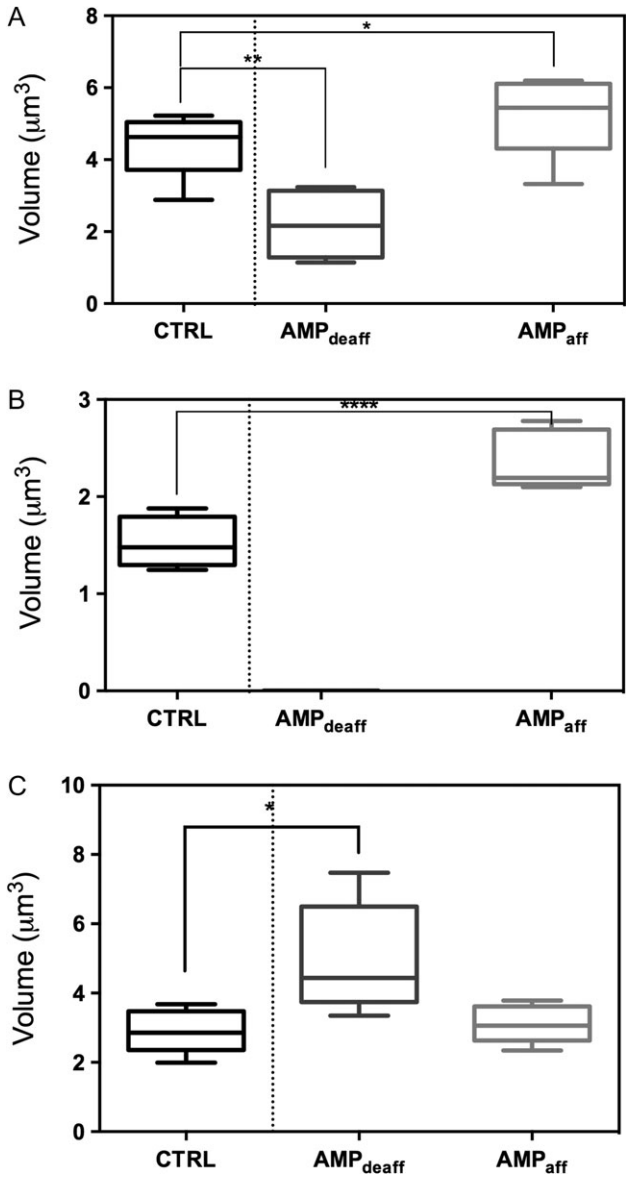

Figure 3. Quantification of the forepaw and lip representation in S1. (A) The reduction in total volume of forepaw S1 representation in AMP_{deaff} hemispheres and its expansion in AMP_{aff} hemispheres. (B) The total volume of the barrels within the S1 forepaw representation. Note that no barrels were found within S1 forepaw representation in AMP_{deaff}, while the volume of barrels within the S1 forepaw representation was bigger in AMP_{aff} as compared with CTRL animals. (C) The expansion of neighboring lip S1 representation in AMP_{deaff}, reaching volumes higher than CTRL and AMP_{aff}. *$P < 0.05$; **$P < 0.01$; ****$P < 0.0001$.

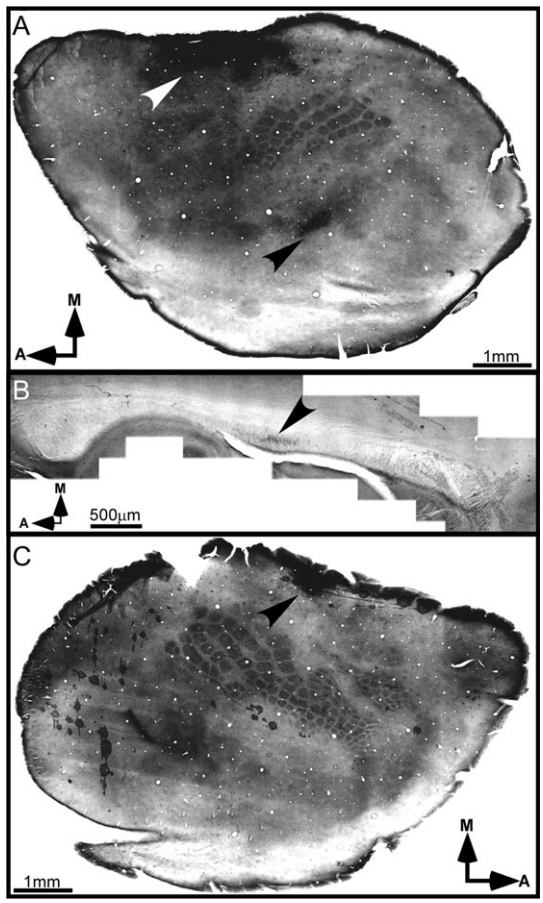

Figure 4. Double labeling of cytochrome oxidase and BDA histochemical reactions in tangential sections. (A) The BDA injection site (white arrowhead) was positioned in the forepaw representation of S1 and a terminal field of ipsilateral corticocortical projections could be discerned in S2 (black arrowhead). (B) A sagittal section of the corpus callosum shows the sector wherein the forepaw callosal axons cross the midline (black arrowhead). (C) A tangential section of the deafferented hemisphere shows the BDA callosal terminal site restricted to the forepaw S1 representation (black arrowhead).

qualitatively in the reconstructions, callosal arbors within AMPaff S1 are enlarged, as compared with CTRL.

Callosal Terminal Arbors are Expanded in the Afferented S1 Cortex of Early-Amputated Animals

The 3D reconstruction of single callosal axon terminals labeled with BDA demonstrated that fibers arriving at the contralateral representation of the forepaw in S1 match the homotopic somatosensory representation in the contralateral hemispheres both in CTRL and AMP animals (Figs 7 and 8).

All 3D reconstructions analyzed showed axon terminals spanning infragranular and supragranular layers in the afferented hemispheres. At all these layers there were synaptic en passant and terminaux boutons (see below).

Table 1 displays a summary of the morphometric parameters measured in 3D reconstructions of callosal axons innervating the representation of forepaw in the contralateral S1 of both AMP and CTRL cases.

Noticeably, all morphometric parameters were larger in the amputated animals (Fig. 9). Additionally, a further analysis of axonal orientation and scattering revealed no changes in axonal orientation, but a change in scattering of callosal axons within the forepaw representation area of S1 in AMP animals (Fig. 10).

Terminal Boutons are More Numerous in Callosal Axons Innervating the Expanded S1 Representation of the Forepaw in the Afferented Hemisphere

Terminal boutons of the callosal axons originating from the forepaw representation in S1 contralateral to the limb amputation (AMP_{deaff}), and situated within the contralateral afferented, homotopic regions of the cortical areas (AMP_{aff}) were present in all cortical layers, except layer I. We found both en passant (Bp) and terminaux (Bt) boutons in the terminal callosal axons labeled

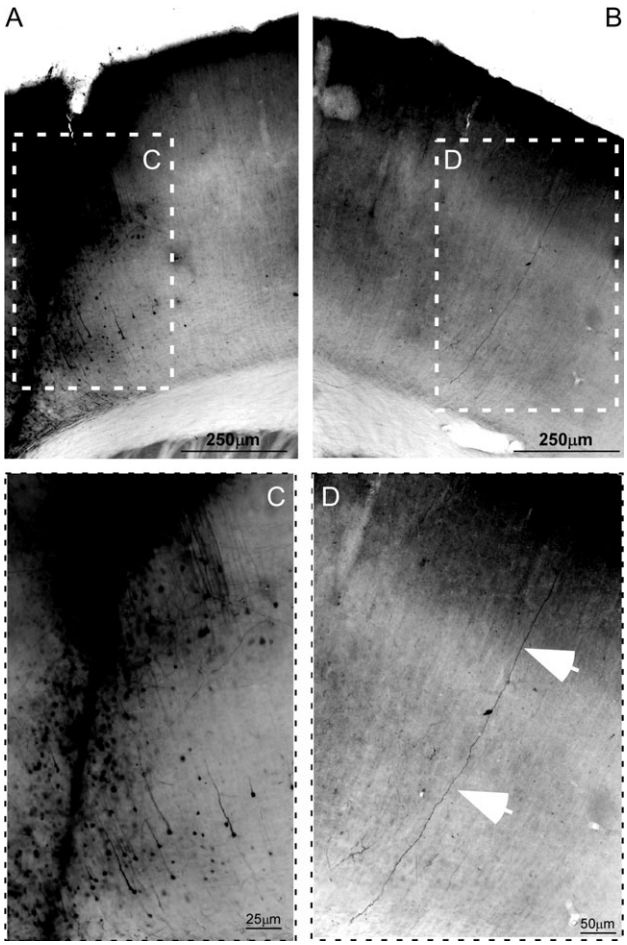

Figure 5. Axonal labeling after BDA injection. (*A*) Coronal section showing injection site at left (notice indentation produced by pipette penetration at the surface) in the deafferented hemisphere. (*B*) The projection field in the afferented hemisphere at homotopic position in the same coronal section. (*A* and *B*) Interrupted rectangles correspond to the enlarged fields below. (*C*) Labeled pyramids appearing at the lower part of the photograph, close to the injection area. (*D*) Enlarged view of the projection field shows a callosal axon (arrowheads) penetrating the cortical layers in the afferented hemisphere.

with BDA. Both the total number of Bp ($t = 7.557$; $P = 0.0001$) and the total number of Bt ($t = 3.289$; $P = 0.008$) were higher in the expanded forepaw representation of AMP_{aff} than in the corresponding hemisphere of CTRL (Fig. 11).

Discussion

Changes in Afferented and Deafferented S1 After Early Forepaw Amputation

To the best of our knowledge, all mammals studied so far present at least 3 complete representations (somatotopic maps) of the contralateral body surface within the cerebral cortex, namely, areas S1, S2, and PV (Kaas 1983; Kaas et al. 1983; Krubitzer and Calford 1992; Inan and Crair 2007; Seelke et al. 2012). S1 has a complete representation of the contralateral half of the animal's body, with a tail-to-face sequential arrangement in the parietal cortex, in such a way that the tail and hindlimb are represented more medially and the face more laterally, with the forelimb and trunk occupying an intermediate position. S2 is located lateral and caudal to S1 and has a less accurate topographic representation

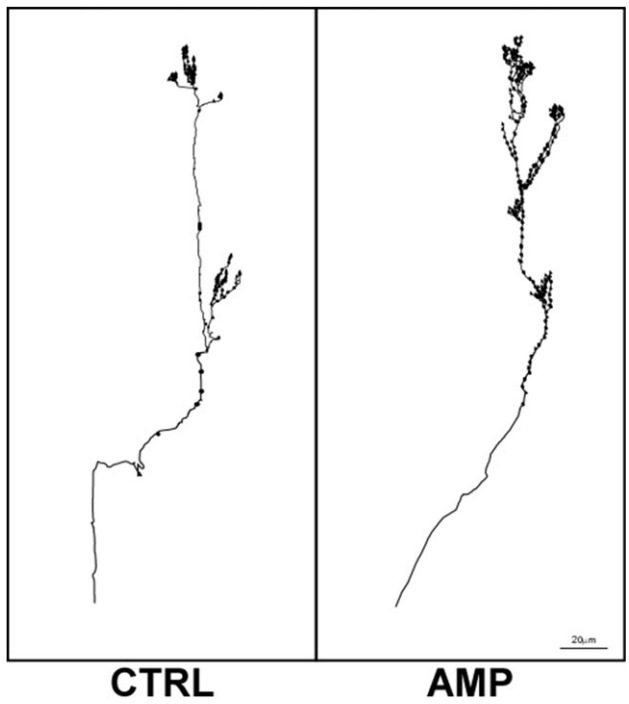

Figure 6. Two examples of reconstructed terminal arbors of single callosal axons originating in the AMP_{deaff} S1 and terminating in the AMP_{aff} homotopic region, contralaterally.

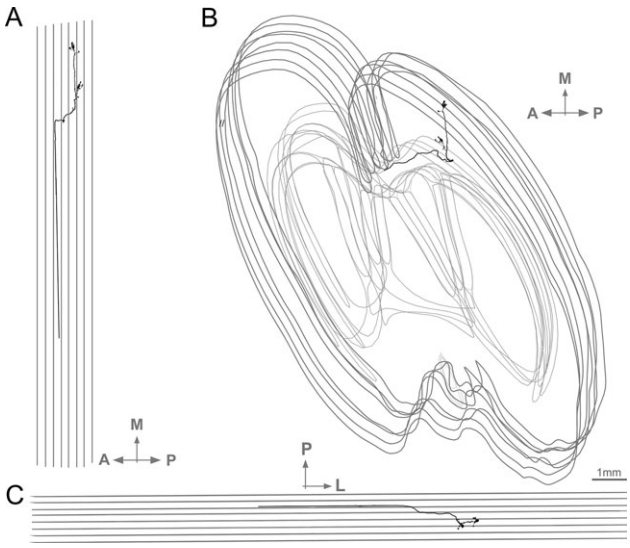

Figure 7. 3D single fiber reconstruction of a callosal axon in a CTRL animal. (*A*) A lateral profile of the callosal axon tree. (*B*) The diagonal view of the same axon, and (*C*) shows its corresponding dorsal view. Note that the axonal tree is restricted to a few sections.

of the contralateral body surface (Beck et al. 1996). There is a third somatosensory representation identified in the parietal region that was called the ventral parietal (PV) area (Krubitzer et al. 1986). We here focused on S1 to investigate morphological plasticity of maps and axons in limb-amputated rats. A peculiar feature of the primary somatosensory cortex is an enlarged representation of some particular regions of the sensory periphery, such as the hands and lips in humans or the large mystacial vibrissae (whiskers) and the forepaw in small rodents (Woolsey

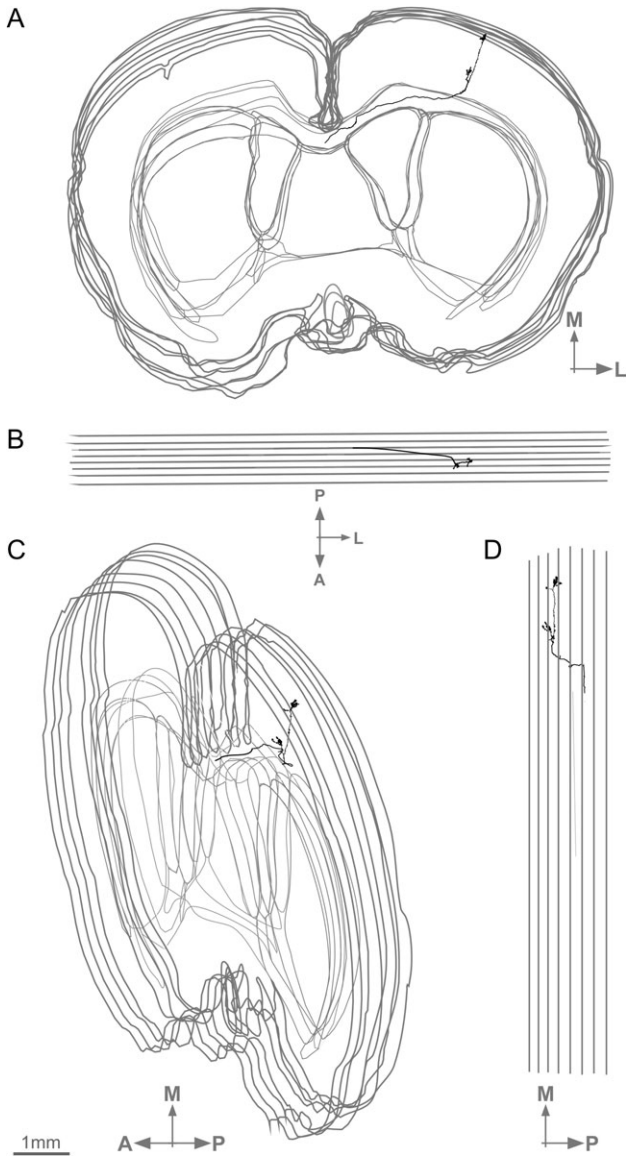

Figure 8. 3D single fiber reconstruction of a callosal axon in a AMP animal. (*A*) A coronal view of the callosal axon tree. (*B*) A dorsal view of the same axon. (*C* and *D*) The corresponding diagonal and lateral views, respectively. Similar to the CTRL animals (Fig. 7), callosal axon trees in early amputated animals are restricted to a few sections.

and Van der Loos 1970; Woolsey 2016). It is believed that this selective cortical magnification is related not only to the density of peripheral innervation, but also to intrinsic cortical factors (Welker and Van der Loos 1986; Catania 1995; Catania and Henry 2006) involving the need for a more sophisticated information processing originated from these body parts.

These topographic representation maps are use-dependent, dynamically maintained, and can be reorganized following brain damage, spinal cord injury or peripheral neural loss (Xerri 2012). These maps can be revealed histochemically by the high activity of cytochrome C oxidase, an enzyme involved in the electron transport chain of the mitochondrial membrane (Wong-Riley and Welt 1980; Land and Simons 1985; Arnold et al. 2001). The development of the barrel fields and the entire rat's body surface representation (so-called "rattunculus") starts at first postnatal day (P1) (first 24 h after birth) and is completed by P4 in S1 (McCandlish et al. 1989). It is conceivable that this early phase of development comprises the critical period for plasticity of the map and axons, as the present results show, but this aspect needs further experiments with a cross-sectional age design. The normal course of development is changed by losses in the sensory periphery such as deafferentation (McCandlish et al. 1996), resulting in anomalous topographic proportions of the body map.

The correspondence between the overall pattern of cytochrome C oxidase labeling and the well-known somatotopic map in S1 is believed to match the major sites of synaptic interactions between thalamic afferents and cortical neurons (White 1978; Feldman et al. 1999) and is subject to changes after early sensory deprivation (Wong-Riley and Welt 1980; Wallace and Fox 1999; Skibinska et al. 2000).

In this work, we aimed to evaluate the representation of the forepaw within S1 under normal conditions and after early forepaw amputation, trying to replicate experimentally at a meso/microscale level the data reported in long-term human amputees (Hamzei et al. 2001; Karl et al. 2001; Simões et al. 2012; Yu et al. 2014; Williams et al. 2016). We showed that in the hemisphere contralateral to the amputation (AMP_{deaff}), the representation of the forepaw in S1 is smaller than in control animals, while the lips are represented in a larger area, as if "invading" the forepaw territory (Fig. 3). This agrees with previous work showing a developmental, time-dependent alteration in the somatotopic map of the deafferented S1 in rodents (Waters et al. 1990; Barrera et al. 2013; Luhmann and Khazipov 2017) and humans (Simões et al. 2012). Further, the representation of the forepaw in S1 within the opposite, afferented hemisphere (AMP_{aff}) was larger than in non-operated animals (Figs 2 and 3), in agreement with our previous work in humans (Simões et al. 2012). Although results agree between rats and humans, a reliable explanation of what happens in human amputees requires the advancement of technologies capable of showing microscale mechanisms in vivo in humans, so far unavailable.

Once sensory information arrives at S1 from the body, it is transferred (or shared) by callosal fibers (Bloom and Hynd 2005) to homologous areas of the contralateral S1 (Krupa et al. 2004; Ferezou et al. 2007), and the same applies to other sensorimotor areas (Chovsepian et al. 2017). Callosal connections provide a dynamic modulation of circuits in each hemisphere, both excitatory and inhibitory (mostly inhibitory: Makarov et al. 2008; van der Knaap and van der Ham 2011). Therefore, it is conceivable that after long-term absence of such crossed modulatory transfer from the silent forepaw region in AMP_{deaff} S1, a reorganization of circuits takes place, provoking an occupation of neighboring regions by axons from the "empty" territory in opposite AMP_{aff} S1, and providing an enlarged input to the forepaw region. Similar macroscale results were found in humans using fMRI (Simões et al. 2012). These data motivated the next issue tackled in this work: do callosal fibers projecting from the smaller forepaw representation in the AMP_{deaff} cerebral hemisphere to the opposite, enlarged representation in AMP_{aff}, show a correspondingly dysmorphic pattern at the single-axon level?

Corticocortical S1 Connections From AMP_{deaff} to AMP_{aff}

All iontophoretic injections of anterograde BDA were targeted to the presumed representation of the forepaw in the deafferented S1, and exhibited a columnar central core surrounded by labeled neuronal cell bodies plus axonal fragments belonging to local intracortical circuits, spanning layers II to VI. Labeled axons could be followed from the forepaw representation in S1

Table 1 Morphometric characteristics of callosal axons in the CTRL and AMP animals

	Amputated (mean ± SD)	Control (mean ± SD)
Area (μm^2)	8.405e+008 (± 6.106e+007)	4.230e+008 (± 7.706e+007)
Volume (μm^3)	2.879e+010 (± 3.318e+009)	2.399e+009 (± 8.170e+008)
Perimeter (μm)	2.180e+008 (± 8.837e+006)	1.481e+008 (± 3.702e+007)
Surface (μm^2)	29 366 (± 1688)	37 921 (± 884.2)
Total number of boutons en Passant	160.8 (± 8.228)	78.00 (± 7.243)
Total number of boutons Terminaux	206.0 (± 21.28)	118.8 (± 15.68)

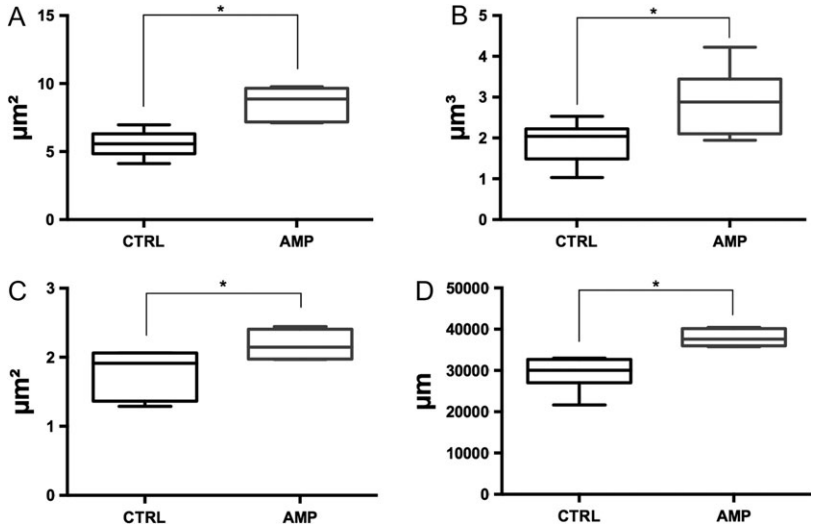

Figure 9. Box-plots of the morphometric analysis of callosal axon trees within the afferented hemisphere. (*A*) Area (μm^2), (*B*) Volume (μm^3), (*C*) Surface (μm^2) and (*D*) Perimeter (μm) of the callosal axon terminals connecting forepaw S1 representations. For all morphometric parameters analyzed, there were statistically significant differences between AMP and CTRL groups. *$P < 0.05$.

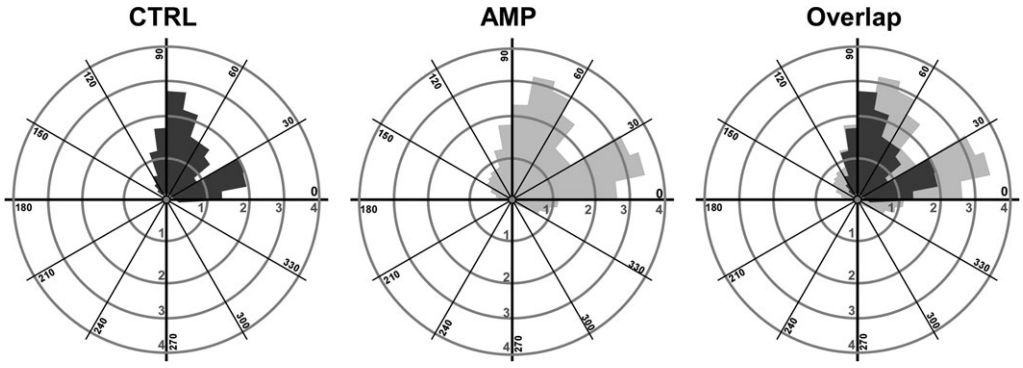

Figure 10. Polar scattering histogram of average axonal tree dispersion of CTRL and AMP. Concentric circles represent 50 (circle 1), 100 (circle 2), 150 (circle 3) and 200 (circle 4) μm, respectively. Bins corresponding to orientations between 0°–120° and 0°–165° were grouped (shown in dark blue for CTRL and light blue for AMP, respectively) and represent the predominant scattering orientation. The overlap shows the difference between CTRL and AMP.

within the AMP_{deaff} cerebral hemisphere until target regions in the ipsilateral hemisphere such as S2, PV, and PR areas (Fig. 4). Additionally, callosal axons could be followed until the homotopic sectors of contralateral S1 (Figs 5–8). This is in accordance with the basic plan of feedforward projections as described by different authors (Coogan and Burkhalter 1993; Alloway 2008), although heterotopic projections do exist in lower numbers (Houzel et al. 2002; Chovsepian et al. 2017).

Callosal connections are often considered as restricted to the midline of sensory fields (Hayama and Ogawa 1997; but see Houzel et al. 2002). Indeed, in S1 particularly, most of the anatomical and functional studies performed so far have demonstrated these corticocortical connections in the corresponding cortical areas of representation of the medial portions of the trunk (Jones and Powell 1968; Akers and Killackey 1978, 1979) with the presumed function of linking the 2 halves of the cortical sensory maps, therefore, unifying the 2 halves of the body (Berlucchi 1972, 1999, 2004, 2012).

However, in S1, callosal connections were found also lateral to the midline (representing the extremities of the limbs), as described in humans (Karol et al. 1970; Maldjian et al. 2014), monkeys (Pandya and Rosene 1993), cats (Conti et al. 1986;

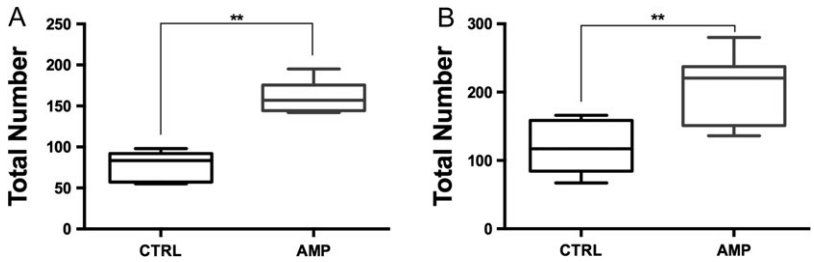

Figure 11. The number of en passant and terminaux boutons. (*A*) Number of en passant boutons (Bp). (*B*) Number of the terminaux boutons (Bt). In both cases, there are more boutons (of both types) in the axonal trees of the AMP_{aff} than in the CTRL groups. $^{**}P < 0.008$.

Manzoni et al. 1986) and, more recently, big rodents as the agouti (Rocha et al. 2007). In rats, callosal connections have been described in the forepaw region as well (Dawson and Killackey 1987; Koralek et al. 1990), besides the whiskers representation (Ferezou et al. 2007). Our results confirm these data and provide qualitative and quantitative descriptions of the fine axonal characteristics in normotypic and early-amputated animals.

Feedforward connections from S1 targeting other somatosensory areas in the parietal cortex of the same side, as well as those in the contralateral cerebral hemisphere in the homotopic S1 have already been described for small rodents (Fabri and Burton 1991; Hayama and Ogawa 1997) and big rodents (Rocha et al. 2007), suggesting that tactile information originating from S1 is processed in parallel in both cerebral hemispheres. This feature supports the argument about the formation of neural assemblies integrated into a functional network of the somatosensory system (Coogan and Burkhalter 1993; Douglas and Martin 2004, 2007; Berger et al. 2009; Singer 2013) and gives support to the hypothesis that callosal axons may be relevant to synchronize electrical activity between both cerebral hemispheres in ways relevant for the dynamic connectivity linking perceptually both halves of the world (Innocenti et al. 1995). In addition, axonal projection into the contralateral cerebral cortex appears to be of great topographic precision by nature, albeit not necessarily independent of previous sensory experience (Iwamura et al. 2001, 2002).

Our results showed the exact location where “forepaw” callosal axons cross the sagittal plane at the corpus callosum: immediately and vertically above the fornix, laterolaterally aligned with S1 area, slightly posterior and superior to the anterior commissure (Fig. 4*B*). Additionally, they confirm the fine topographic organization of interhemispheric axons at the corpus callosum (Pandya et al. 1971; Bozhko and Slepchenko 1988; Doron and Gazzaniga 2008), and provide topographic information relevant for ultrastructural studies in the callosum, as approached in other studies of our group (Vianna-Barbosa et al. 2017).

Morphometric Analysis of S1 Forepaw Callosal Axons Show Arbor Expansion After Amputation

In this work, we were able to reconstruct and analyze quantitatively single callosal axons that connect the forepaw regions in S1 of normotypic and early amputated (P0) animals, aiming to explain at a single-axon level the previous findings of forelimb topographic changes within the somatosensory cortex of amputees. Our results built upon previous work on partial axonal branches (De Paola et al. 2006), revealing the whole 3D morphology of forepaw callosal axons and their arborizations in all cortical layers (except layer I). Similar work was done for ipsilateral corticocortical and thalamocortical axons in the normal rat brain (Oberlaender et al. 2011; 2012).

Our 3D reconstruction analysis showed significant increases in microstructural parameters such as area, perimeter, and surface area, volume, and axonal tree scatter in the early amputated animals as compared with controls (Figs 9 and 10). Additionally, we showed that the number of en passant and terminaux boutons was larger in the early-amputated animals than in the controls (Fig. 11).

Axons were selected for reconstruction according to the completeness of labeling from the midline to the terminal field with its boutons. This criterion to select the sample makes it randomized in terms of layers of origin and callosal neuron subtypes. But, on the other hand, it creates a potential limitation by assuming that plasticity after deafferentation impacts similarly all callosal neurons. This hypothesis, however, is unlikely, since the morphological differences found between experimental groups were very significant for all the quantified parameters of the axonal arbors.

Stabilization of neural connectivity during postnatal critical periods is activity-dependent and makes use of the activation patterns to adjust the strength and number of synaptic connections (Changeux and Danchin 1976; Lubke et al. 2003; Maffei and Turrigiano 2008). Also, during this developmental phase, a very large number of synapses are formed (Rakic et al. 1986). Thus, it is conceivable that the microscale axonal changes found in amputated animals were consequences of the early sensory deprivation, imposed during the critical period of postnatal development, that resulted in a less pronounced pruning usually attributed to experience-dependent plasticity (Abbott and Nelson 2000; Gogolla et al. 2007). This interpretation dates back to the seminal work of Innocenti and collaborators (Innocenti et al. 1977, 1995; Aggoun-Zouaoui et al. 1996) who discovered that callosal neurons, as well as their axons and terminals in newborn animals outnumber those in adults, being pruned along development under the influence of environmental cues. Direct, quantitative evidence for exuberance followed by pruning of callosal fibers at the midline has been produced for cats (Berbel and Innocenti 1988) and for primates (LaMantia and Rakic 1990), suggesting that this kind of plasticity could be a general developmental phenomenon in mammals. Sensory deprivation during early postnatal development, when axonal telodendria are being formed and refined (Fenlon and Richards 2015), makes callosal axon arbors asymmetrical between both cerebral hemispheres (Broser et al. 2008). It is also conceivable that differences between normal and amputated callosal axon morphology is associated to the expansion of forepaw representation in the AMP_{aff} hemisphere after early limb amputation.

During synaptic formation and elimination, boutons are highly plastic structures that strongly contribute to the remodeling of

specific functional circuits and can therefore have a great impact on circuit plasticity of the whole brain (De Paola et al. 2006). Morphologically, they can be classified as en passant boutons (Bp) and terminaux boutons (Bt), both associated with excitatory synapses (McGuire et al. 1984; Anderson and Martin 2001; Anderson et al. 2002). Moreover, boutons addition or subtraction are likely associated to synapse formation or elimination, respectively. It is conceivable, thus, that the increase in the number of Bp and Bt in the afferented S1 cerebral hemisphere (Fig. 11) may be related to the enlarged forepaw representation therein (Figs 2 and 3), providing it with a greater number of callosal synapses for compensatory modulation of activity after amputation. What happens with reciprocal callosal axons that connect the forepaw representation of the afferented cerebral hemisphere to the deafferented side remains unknown.

There is evidence for widespread, continuous structural plasticity of boutons located along terminal arbors, mediating large-scale synaptogenesis, a phenomenon most pronounced during critical periods (Gogolla et al. 2007). Since our data showed an increase in the number of boutons (both Bp and Bt), we can assume that it is a consequence of early amputation, and therefore of the resulting sensory deprivation of S1 neurons contralateral to amputation, which now respond to other inputs from neighboring regions of the body surface cortical representation (Arnold et al. 2001). The consequences are the increase of the forepaw S1 representation within the afferented cerebral hemisphere and a parallel increase in callosal axon scatter, as shown in Figure 10.

Conclusions

We have shown that early amputation of the forepaw in rats induces a reduction in its representation within S1 of the deafferented cerebral hemisphere (contralateral to the amputation), but provokes an enlargement in the afferented side (ipsilateral to the amputation). In addition, microstructural changes take place in callosal axons from neurons of the reduced deafferented side which innervate the expanded forepaw representation on the afferented S1. Consistently, all measures of single axons such as scatter of terminal arbors, as well as volume, area and perimeter, display significant increases, together with the number of terminal boutons. We hypothesize that the expansion of the cortical field requires an equivalent expansion in callosal axon innervation in order to compensate for the imbalance created by early limb amputation. These changes can be attributed to experience-dependent plasticity, which characterizes synaptic development during the critical period, as described in the somatosensory cortex (Wise and Jones 1976; Foeller and Feldman 2004; Mizuno et al. 2007) after early sensory deprivation.

Funding

Conselho Nacional de Desenvolvimento Científico e Tecnológico (CNPq, Grant 470734/2012-4 to R.L.; CNPq, Grant 150959/2014-1 and 447835/2014-9 to C.P.B.); Fundação de Amparo à Pesquisa do Estado do Rio de Janeiro (FAPERJ, Grant 010.002983/2014 to R.L.); and Instituto Nacional de Neurociência Translacional (INNT, Grant 465346/2014-6 to R.L.)

Notes

We thank the students Nicole Correa da Costa and Alexandre Gnattali Sanabio for help in some of the experiments. The technical assistance of Camila Madeiro Lopes and Camila Gomes da Silva is also acknowledged. *Conflict of interest*: None declared.

References

Abbott LF, Nelson SB. 2000. Synaptic plasticity: taming the beast. Nat Neurosci. 3(Suppl):1178–1183.

Aboitiz F, Scheibel AB, Fisher RS, Zaidel E. 1992a. Fiber composition of the human corpus callosum. Brain Res. 598:143–153.

Aboitiz F, Scheibel AB, Fisher RS, Zaidel E. 1992b. Individual differences in brain asymmetries and fiber composition in the human corpus callosum. Brain Res. 598:154–161.

Aggoun-Zouaoui D, Kiper DC, Innocenti GM. 1996. Growth of callosal terminal arbors in primary visual areas of the cat. Eur J Neurosci. 8:1132–1148.

Aguiar P, Souza M, Szucs P. 2013. Versatile morphometric analysis and visualization of the three-dimensional structure of neurons. Neuroinform. 11:393–403.

Akers RM, Killackey HP. 1978. Organization of corticocortical connections in the parietal cortex of the rat. J Comp Neurol. 181:513–537.

Akers RM, Killackey HP. 1979. Segregation of cortical and trigeminal afferents to the ventrobasal complex of the neonatal rat. Brain Res. 161:527–532.

Alloway KD. 2008. Information processing streams in rodent barrel cortex: the differential functions of barrel and septal circuits. Cer Cortex. 18:979–989.

Anderson JC, Binzegger T, Douglas RJ, Martin KA. 2002. Chance or design? Some specific considerations concerning synaptic boutons in cat visual cortex. J Neurocytol. 31:211–229.

Anderson JC, Martin KA. 2001. Does bouton morphology optimize axon length? Nat Neurosci. 4:1166–1167.

Arnold PB, Li CX, Waters RS. 2001. Thalamocortical arbors extend beyond single cortical barrels: an in vivo intracellular tracing study in rat. Exp Brain Res. 136:152–168.

Barrera K, Chu P, Abramowitz J, Steger R, Ramos RL, Brumberg JC. 2013. Organization of myelin in the mouse somatosensory barrel cortex and the effects of sensory deprivation. Dev Neurobiol. 73:297–314.

Beck PD, Pospichal MW, Kaas JH. 1996. Topography, architecture, and connections of somatosensory cortex in opossums: evidence for five somatosensory areas. J Comp Neurol. 366: 109–133.

Berbel P, Innocenti GM. 1988. The development of the corpus callosum in cats: a light- and electron-microscopic study. J Comp Neurol. 276:132–156.

Berger TK, Perin R, Silberberg G, Markram H. 2009. Frequency-dependent disynaptic inhibition in the pyramidal network: a ubiquitous pathway in the developing rat neocortex. J Physiol. 587:5411–5425.

Berlucchi G. 1972. Anatomical and physiological aspects of visual functions of corpus callosum. Brain Res. 37:371–392.

Berlucchi G. 1999. Integration of brain activities: the roles of the diffusely projecting brainstem systems and the corpus callosum. Brain Res Bull. 50:389–390.

Berlucchi G. 2004. Some effects of cortical and callosal damage on conscious and unconscious processing of visual information and other sensory inputs. Prog Brain Res. 144:79–93.

Berlucchi G. 2012. Frontal callosal disconnection syndromes. Cortex. 48:36–45.

Bloom JS, Hynd GW. 2005. The role of the corpus callosum in interhemispheric transfer of information: excitation or inhibition? Neuropsychol Rev. 15:59–71.

Bowlus TH, Lane RD, Stojic AS, Johnston M, Pluto CP, Chan M, Chiaia NL, Rhoades RW. 2003. Comparison of reorganization of the somatosensory system in rats that sustained forelimb removal as neonates and as adults. J Comp Neurol. 465:335–348.

Bozhko GT, Slepchenko AF. 1988. Functional organization of the callosal connections of the cat auditory cortex. Neurosci Behav Physiol. 18:323–330.

Broser P, Grinevich V, Osten P, Sakmann B, Wallace DJ. 2008. Critical period plasticity of axonal arbors of layer 2/3 pyramidal neurons in rat somatosensory cortex: layer-specific reduction of projections into deprived cortical columns. Cereb Cortex. 18:1588–1603.

Buonomano DV, Merzenich MM. 1998. Cortical plasticity: from synapses to maps. Ann Rev Neurosci. 21:149–186.

Caminiti R, Innocenti GM, Manzoni T. 1979. The anatomical substrate of callosal messages from SI and SII in the cat. Exp Brain Res. 35:295–314.

Catania KC. 1995. Magnified cortex in star-nosed moles. Nature. 375:453–454.

Catania KC. 2005. Star-nosed moles. Curr Biol. 15:R863–R864.

Catania KC, Henry EC. 2006. Touching on somatosensory specializations in mammals. Curr Opin Neurobiol. 16:467–473.

Changeux JO, Danchin A. 1976. Selective stabilization of developing synapses as a mechanism for the specification of neuronal networks. Nature. 264:705–712.

Chen LM, Qi HX, Kaas JH. 2012. Dynamic reorganization of digit representations in somatosensory cortex of nonhuman primates after spinal cord injury. J Neurosci. 32:14649–14663.

Chovsepian A, Empl L, Correa D, Bareyre FM. 2017. Heterotopic transcallosal projections are present throughout the mouse cortex. Front Cell Neurosci. 11:36.

Conti F, Fabri M, Manzoni T. 1986. Bilateral receptive fields and callosal connectivity of the body midline representation in the first somatosensory area of primates. Somatosens Res. 3:273–289.

Coogan TA, Burkhalter A. 1993. Hierarchical organization of areas in rat visual cortex. J Neurosci. 13:3749–3772.

Dawson DR, Killackey HP. 1987. The organization and mutability of the forepaw and hindpaw representations in the somatosensory cortex of the neonatal rat. J Comp Neurol. 256:246–256.

De Paola V, Holtmaat A, Knott G, Song S, Wilbrecht L, Caroni P, Svoboda K. 2006. Cell type-specific structural plasticity of axonal branches and boutons in the adult neocortex. Neuron. 49:861–875.

Doron KW, Gazzaniga MS. 2008. Neuroimaging techniques offer new perspectives on callosal transfer and interhemispheric communication. Cortex. 44:1023–1029.

Douglas RJ, Martin KA. 2004. Neuronal circuits of the neocortex. Ann Rev Neurosci. 27:419–451.

Douglas RJ, Martin KA. 2007. Recurrent neuronal circuits in the neocortex. Curr Biol. 17:R496–R500.

Fabri M, Burton H. 1991. Topography of connections between primary somatosensory cortex and posterior complex in rat: a multiple fluorescent tracer study. Brain Res. 538:351–357.

Feldman DE, Nicoll RA, Malenka RC. 1999. Synaptic plasticity at thalamocortical synapses in developing rat somatosensory cortex: LTP, LTD, and silent synapses. J Neurobiol. 41:92–101.

Fenlon LR, Richards LJ. 2015. Contralateral targetinf of the corpus callosum in normal and pathological brain funcion. Trends Neurosci. 38:264–272.

Ferezou I, Haiss F, Gentet LJ, Aronoff R, Weber B, Petersen CC. 2007. Spatiotemporal dynamics of cortical sensorimotor integration in behaving mice. Neuron. 56:907–923.

Foeller E, Feldman DE. 2004. Synaptic basis for developmental plasticity in somatosensory cortex. Curr Opin Neurobiol. 14:89–95.

Fox K. 2002. Anatomical pathways and molecular mechanisms for plasticity in the barrel cortex. Neuroscience. 111:799–814.

Gogolla N, Galimberti I, Caroni P. 2007. Structural plasticity of axon terminals in the adult. Curr Opin Neurobiol. 17:516–524.

Hamzei F, Liepert J, Dettmers C, Adler T, Kiebel S, Rijntjes M, Weiller C. 2001. Structural and functional cortical abnormalities after upper limb amputation during childhood. Neuroreport. 12:957–962.

Hayama T, Ogawa H. 1997. Regional differences of callosal connections in the granular zones of the primary somatosensory cortex in rats. Brain Res Bull. 43:341–347.

Houzel J-C, Carvalho ML, Lent R. 2002. Interhemispheric connections between primary visual areas: beyond the midline rule. Braz J Med Biol Res. 35:1441–1453.

Hua XY, Li ZY, Xu WD, Zheng MX, Xu JG, Gu YD. 2012. Interhemispheric functional reorganization after cross nerve transfer: via cortical or subcortical connectivity? Brain Res. 1471:93–101.

Inan M, Crair MC. 2007. Development of cortical maps: perspectives from the barrel cortex. Neuroscientist. 13:49–61.

Innocenti GM. 2009. Dynamic interactions between the cerebral hemispheres. Exp Brain Res. 192:417–423.

Innocenti GM, Aggoun-Zouaoui D, Lehmann P. 1995. Cellular aspects of callosal connections and their development. Neuropsychologia. 33:961–987.

Innocenti GM, Fiore L, Caminiti R. 1977. Exuberant projection into the corpus callosum from the visual cortex of newborn cats. Neurosci Lett. 4:237–242.

Ivy GO, Akers RM, Killackey HP. 1979. Differential distribution of callosal projection neurons in the neonatal and adult rat. Brain Res. 173:532–537.

Iwamura Y, Tanaka M, Iriki A, Taoka M, Toda T. 2002. Processing of tactile and kinesthetic signals from bilateral sides of the body in the postcentral gyrus of awake monkeys. Behav Brain Res. 135:185–190.

Iwamura Y, Taoka M, Iriki A. 2001. Bilateral activity and callosal connections in the somatosensory cortex. Neuroscientist. 7:419–429.

Jones EG, Powell TP. 1968. The commissural connexions of the somatic sensory cortex in the cat. J Anat. 103:433–455.

Kaas JH. 1983. What, if anything, is SI? Organization of first somatosensory area of cortex. Physiol Rev. 63:206–231.

Kaas JH, Merzenich MM, Killackey HP. 1983. The reorganization of somatosensory cortex following peripheral nerve damage in adult and developing mammals. Ann Rev Neurosci. 6:325–356.

Karl A, Birbaumer N, Lutzenberger W, Cohen LG, Flor H. 2001. Reorganization of motor and somatosensory cortex in upper extremity amputees with phantom limb pain. J Neurosci. 21:3609–3618.

Karol EA, Heilbronn D, Pandya D. 1970. The termination of callosal fibers in the rhesus monkey. Trans Am Neurol Assoc. 95:269–271.

Koralek KA, Olavarria J, Killackey HP. 1990. Areal and laminar organization of corticocortical projections in the rat somatosensory cortex. J Comparative Neurol. 299:133–150.

Krubitzer LA, Calford MB. 1992. Five topographically organized fields in the somatosensory cortex of the flying fox: microelectrode maps, myeloarchitecture, and cortical modules. J Comp Neurol. 317:1–30.

Krubitzer LA, Sesma MA, Kaas JH. 1986. Microelectrode maps, myeloarchitecture, and cortical connections of three somatotopically organized representations of the body surface in the parietal cortex of squirrels. J Comp Neurol. 250:403–430.

Krupa DJ, Wiest MC, Shuler MG, Laubach M, Nicolelis MA. 2004. Layer-specific somatosensory cortical activation during active tactile discrimination. Science. 304:1989–1992.

LaMantia A-S, Rakic P. 1990. Axon overproduction and elimination in the corpus callosum of the developing rhesus monkey. J Neurosci. 10:2156–2175.

Land PW, Simons DJ. 1985. Cytochrome oxidase staining in the rat SmI barrel cortex. J Comp Neurol. 238:225–235.

Lane RD, Bennett-Clarke CA, Chiaia NL, Killackey HP, Rhoades RW. 1995. Lesion-induced reorganization in the brainstem is not completely expressed in somatosensory cortex. Proc Natl Acad Sci USA. 92:4264–4268.

Lee HK, Whitt JL. 2015. Cross-modal synaptic plasticity in adult primary sensory cortices. Curr Opin Neurobiol. 35:119–126.

Lent R, Tovar-Moll F. 2015. How can development and plasticity contribute to understanding evolution of the human brain? Front Hum Neurosci. 9:208.

Lubke J, Roth A, Feldmeyer D, Sakmann B. 2003. Morphometric analysis of the columnar innervation domain of neurons connecting layer 4 and layer 2/3 of juvenile rat barrel cortex. Cereb Cortex. 13:1051–1063.

Luhmann HJ, Khazipov R. 2017. Neuronal activity patterns in the developing barrel cortex. Neuroscience. doi:10.1016/j.neuroscience.2017.05.025.

Maffei A, Turrigiano G. 2008. The age of plasticity: developmental regulation of synaptic plasticity in neocortical microcircuits. Progr Brain Res. 169:211–223.

Makarov VA, Schmidt KE, Castellanos NP, Lopez-Aguado L, Innocenti GM. 2008. Stimulus-dependent interaction between the visual areas 17 and 18 of the 2 hemispheres of the ferret (*Mustela putorius*). Cereb Cortex. 18:1951–1960.

Maldjian JA, Davenport EM, Whitlow CT. 2014. Graph theoretical analysis of resting-state MEG data: identifying interhemispheric connectivity and the default mode. NeuroImage. 96:88–94.

Maldjian JA, Gottschalk A, Patel RS, Detre JA, Alsop DC. 1999. The sensory somatotopic map of the human hand demonstrated at 4 Tesla. NeuroImage. 10:55–62.

Manzoni T, Conti F, Fabri M. 1986. Callosal projections from area SII to SI in monkeys: anatomical organization and comparison with association projections. J Comp Neurol. 252:245–263.

McCandlish CA, Li CX, Waters RS, Howard EM. 1996. Digit removal leads to discrepancies between the structural and functional organization of the forepaw barrel subfield in layer IV of rat primary somatosensory cortex. Exp Brain Res. 108:417–426.

McCandlish C, Waters RS, Cooper NG. 1989. Early development of the representation of the body surface in SI cortex barrel field in neonatal rats as demonstrated with peanut agglutinin binding: evidence for differential development within the rattunculus. Exp Brain Res. 77:425–431.

McGuire BA, Stevens JK, Sterling P. 1984. Microcircuitry of bipolar cells in cat retina. J Neurosci. 4:2920–2938.

Mizuno H, Hirano T, Tagawa Y. 2007. Evidence for activity-dependent cortical wiring: formation of interhemispheric connections in neonatal mouse visual cortex requires projection neuron activity. J Neurosci. 27:6760–6770.

Oberlaender M, Boudewijns ZS, Kleele T, Mansvelder HD, Sakmann B, de Kock CP. 2011. Three-dimensional axon morphologies of individual layer 5 neurons indicate cell type-specific intracortical pathways for whisker motion and touch. Proc Natl Acad Sci USA. 108:4188–4193.

Oberlaender M, de Kock CP, Bruno RM, Ramirez A, Meyer HS, Dercksen VJ, Helmstaedter M, Sakmann B. 2012. Cell type-specific three-dimensional structure of thalamocortical circuits in a column of rat vibrissal cortex. Cereb Cortex. 22:2375–2391.

Pandya DN, Karol EA, Heilbronn D. 1971. The topographical distribution of interhemispheric projections in the corpus callosum of the rhesus monkey. Brain Res. 32:31–43.

Pandya DN, Rosene DL. 1993. Laminar termination patterns of thalamic, callosal, and association afferents in the primary auditory area of the rhesus monkey. Exp Neurol. 119:220–234.

Paxinos G, Watson C. 2007. The rat brain in stereotaxic coordinates. Amsterdam: Academic Press/Elsevier.

Paxinos G, Watson CR, Emson PC. 1980. AChE-stained horizontal sections of the rat brain in stereotaxic coordinates. J Neurosci Methods. 3:129–149.

Payne BR. 1996. Reversible deactivation of cerebral network components. Trends Neurosci. 19:535–542.

Pelled G, Chuang KH, Dodd SJ, Koretsky AP. 2007. Functional MRI detection of bilateral cortical reorganization in the rodent brain following peripheral nerve deafferentation. NeuroImage. 37:262–273.

Petersen CC. 2007. The functional organization of the barrel cortex. Neuron. 56:339–355.

Rakic P, Bourgeois JP, Eckenhoff MF, Zecevic N, Goldman-Rakic PS. 1986. Concurrent overproduction of synapses in diverse regions of the primate cerebral cortex. Science. 232:232–235.

Ramachandran VS, Rogers-Ramachandran D, Stewart M. 1992. Perceptual correlates of massive cortical reorganization. Science. 258:1159–1160.

Rocha EG, Santiago LF, Freire MA, Gomes-Leal W, Dias IA, Lent R, Houzel JC, Franca JG, Pereira A Jr., Picanco-Diniz CW. 2007. Callosal axon arbors in the limb representations of the somatosensory cortex (SI) in the agouti (Dasyprocta primnolopha). J Comp Neurol. 500:255–266.

Seelke AM, Dooley JC, Krubitzer LA. 2012. The emergence of somatotopic maps of the body in S1 in rats: the correspondence between functional and anatomical organization. PLoS One. 7:e32322.

Shu SY, Ju G, Fan LZ. 1988. The glucose oxidase-DAB-nickel method in peroxidase histochemistry of the nervous system. Neurosci Lett. 85:169–171.

Simões EL, Bramati I, Rodrigues E, Franzoi A, Moll J, Lent R, Tovar-Moll F. 2012. Functional expansion of sensorimotor representation and structural reorganization of callosal connections in lower limb amputees. J Neurosci. 32:3211–3220.

Singer W. 2013. Cortical dynamics revisited. Trends Cognit Sci. 17:616–626.

Skibinska A, Glazewski S, Fox K, Kossut M. 2000. Age-dependent response of the mouse barrel cortex to sensory deprivation: a 2-deoxyglucose study. Exp Brain Res. 132:134–138.

Staudt M, Gerloff C, Grodd W, Holthausen H, Niemann G, Krageloh-Mann I. 2004. Reorganization in congenital hemiparesis acquired at different gestational ages. Ann Neurol. 56:854–863.

Suarez R, Fenlon LR, Marek R, Avitan L, Sah P, Goodhill GJ, Richards LJ. 2014. Balanced interhemispheric cortical activity is required for correct targeting of the corpus callosum. Neuron. 82:1289–1298.

van der Knaap LJ, van der Ham IJ. 2011. How does the corpus callosum mediate interhemispheric transfer? A review. Behav Brain Res. 223:211–221.

Vianna-Barbosa RJ, Bahia CP, Sanabio AG, Miranda K, Lent R, Tovar-Moll F 2017. Morphological neuroplasticity of somatosensory cortex and its efferents in an animal model of forelimb amputation. *The Brains Conferences—FENS*. Copenhagen, Denmark. http://www.fens.org/Global/Pages/Fall%20BC%202017/Programme_11%20Sept.%202017.pdf

Wallace H, Fox K. 1999. The effect of vibrissa deprivation pattern on the form of plasticity induced in rat barrel cortex. Somatosens Motor Res. 16:122–138.

Waters RS, McCandlish CA, Cooper NG. 1990. Early development of SI cortical barrel subfield representation of forelimb in normal and deafferented neonatal rat as delineated by peroxidase conjugated lectin, peanut agglutinin (PNA). Exp Brain Res. 81:234–240.

Welker E, Van der Loos H. 1986. Quantitative correlation between barrel-field size and the sensory innervation of the whiskerpad: a comparative study in six strains of mice bred for different patterns of mystacial vibrissae. J Neurosci. 6: 3355–3373.

White EL. 1978. Identified neurons in mouse Sml cortex which are postsynaptic to thalamocortical axon terminals: a combined Golgi-electron microscopic and degeneration study. J Comp Neurol. 181:627–661.

Williams L, Pirouz N, Mizelle JC, Cusack W, Kistenberg R, Wheaton LA. 2016. Remodeling of cortical activity for motor control following upper limb loss. Clin Neurophysiol. 127: 3128–3134.

Wise SP, Jones EG. 1976. The organization and postnatal development of the commissural projection of the rat somatic sensory cortex. J Comp Neurol. 168:313–343.

Wong-Riley MT. 1989. Cytochrome oxidase: an endogenous metabolic marker for neuronal activity. Trends Neurosci. 12:94–101.

Wong-Riley MT, Welt C. 1980. Histochemical changes in cytochrome oxidase of cortical barrels after vibrissal removal in neonatal and adult mice. Proc Natl Acad Sci USA. 77:2333–2337.

Woolsey TA. 2016. Re: Woolsey TA, van der Loos H. 1970. The structural organization of layer IV in the somatosensory region (SI) of mouse cerebral cortex. Brain Res. 17: 205–242. Brain Res. 1645:22–24.

Woolsey TA, Van der Loos H. 1970. The structural organization of layer IV in the somatosensory region (SI) of mouse cerebral cortex. The description of a cortical field composed of discrete cytoarchitectonic units. Brain Res. 17:205–242.

Xerri C. 2012. Plasticity of cortical maps: multiple triggers for adaptive reorganization following brain damage and spinal cord injury. Neuroscientist. 18:133–148.

Yu XJ, He HJ, Zhang QW, Zhao F, Zee CS, Zhang SZ, Gong XY. 2014. Somatotopic reorganization of hand representation in bilateral arm amputees with or without special foot movement skill. Brain Res. 1546:9–17.